IMPEDANCE SPECTROSCOPY IN THE SI-HF SYSTEM INCLUDING TIME DEPENDENT AND RESONANT PHENOMENA

G. Hasse, J. Carstensen, and H. Föll
Faculty of Engineering, University of Kiel
Kaiserstr. 2, 24143 Kiel, Germany

ABSTRACT

The Si-HF system exhibits a complicated *I-U*-characteristics and phenomena as e.g., current or voltage oscillations and pore formation, not yet fully understood. Results from current transient measurements, FFT impedance spectroscopy, and novel resonance experiments from all parts of the characteristics (including voltage oscillations) are presented and interpreted in terms of the current burst model. Resonant behavior in parts of the characteristics, voltage oscillations, the peculiar role of inflection points, and the general dominance of oxide formation is investigated; the results tend to support the model.

INTRODUCTION

Starting with the discovery of macroporous (1, 2) and microporous silicon (3-5) the Si-HF system has become increasingly interesting for scientists and engineers. Promising applications are proposed with increasing frequency but in spite of this the system itself is not very well understood – even the *I-U*-characteristics of Fig. 1 with two pronounced peaks (referred to as I_{PSL} and I_{Ox} peaks) still remains somewhat mysterious.

In this paper results from current transient measurements, FFT impedance spectroscopy, and novel resonance experiments from all parts of the characteristics including voltage oscillations are presented and interpreted in terms of the current burst model (6-9).

EXPERIMENTAL

For the experiments an electrochemical PVC cell with two reference electrodes was used. The electrolyte was cycled through the cell by a peristaltic pump and the temperature was controlled by a Julabo thermostat. The potentiostat/ galvanostat was *custom built* with an integrated signal generator producing 43 frequencies with nonharmonic relations spanning an adjustable range from 0.01 mHz to 40 kHz. This allows simultaneous measurements of the response for many frequencies and thus in-situ FFT-impedance spectroscopy (10, 11). The samples were p-Si with a resistance of (1-10) Ωcm contacted with InGa alloy, and the electrolyte was a 0.05 w% HF solution with NH_4Cl salt to reduce the electrolyte resistance. The current transient signal was smoothed by a Stanford SR640 filter which is an integral part of the FFT impedance spectrometer. For the resonance experiments a Hewlett Packard 33120 A waveform generator was used.

CURRENT TRANSIENT MEASUREMENTS

After switching from an anodic potential to open circuit potential (i.e. keeping the circuit closed but without external current flow) any oxide present is dissolved purely chemically by the HF containing electrolyte. The etch front will eventually reach the interface between oxide and the silicon substrate; depending on the local oxide thickness and dissolution kinetics this will locally happen at different times after the potential switching for a inhomogeneous oxide. The interface contains a thin intermediate layer of so called suboxide (12) with the composition $SiO_{(2-x)}$ and there has to be an electrochemical oxidation step before it can be etched. This oxidation requires carrier transfer which can be measured as a transient current in the external circuit producing an $I(t)$-curve called current transient.

The current transients may contain other components too (e.g. charge needed for H coverage (13)) but essentially yields information about the oxide coverage (as only oxidized areas can have a suboxide and therefore produce current) and the oxide thickness distribution. The latter is contained in the shape of the transient peaks as shown in Ref. (14-16). A wide transient peak signifies a broad oxide thickness distribution and the center of gravity of the current transient is a measure for the mean oxide thickness.

FFT-IMPEDANCE SPECTROSCOPY

Impedance spectroscopy analyzes the system behavior in response to small electrical signals. If the conditions of linearity and stationarity are met, the impedance spectrum of the analyzed system can be obtained by adding a voltage (current) signal to a constant voltage (current) in the potentiostatic (galvanostatic) mode and by measuring the current (voltage) response. The ratio of these quantities is the electrical impedance and is generally depending on the frequency. The resulting impedance spectra can be fitted by using appropriate equivalent circuits, consisting of resistors, capacitors, etc., and by this the measured system can be accessed.

The signal used should be as small as possible to maintain linearity but strong enough for a sufficient signal to noise ratio.

Stationarity often is the more important condition for Si measurements, implying that the system does not change during the measurement. The current or voltage oscillations observed with Si samples obviously violate this condition as does pore etching (in principle, though not necessarily in reality). Measurements thus must be fast and the use of a FFT impedance spectrometer is mandatory. The response for frequencies is measured simultaneously and evaluated by the FFT algorithm. The time for one measurement thus is only the time needed to go through some cycles of the lowest frequency.

Another important advantage of the FFT spectrometers is the implicit assessment of non-linearity. If there is noise in the system (or other sources of non-linearity), frequencies will occur in the response that were not contained in the perturbation signal. For standard impedance measurements these frequencies are disregarded.

CURRENT TRANSIENT MEASUREMENTS IN THE ELECTROPOLISHING REGIME

The part of the *I*-*U*-characteristics between the PSL-peak and the oscillations regime will be call "electropolishing regime" and current transient measurements were performed at all accessible voltages. The switch to open circuit potential was performed after the system maintained a constant current for the voltage chosen (which may necessitate an appreciable waiting time). The steady state characteristics then can be constructed by plotting these equilibrium currents versus the voltage. The experimental results in Fig. 2 show first an increase in the suboxide charge Q as obtained by integrating the transient $I(t)$-peak with the voltage, until a maximum is reached and the $Q(U)$ curve decreases again. The maximum corresponds to the point of inflection C on the ascending part to I_{ox} of the I-U-curve in Fig. 1.

Since the transient currents relate directly to the degree of oxide coverage, it should be complete at the point of inflection (about 1V). While it is straight forward to assume that oxide coverage does indeed increase with increasing voltage, the decrease of $Q(U)$ for increasing voltages is just an artifact of the transient measurement (17) indicating that a strongly increasing number of current bursts nucleates through thick oxide layers.

At the point of inflection the curvature changes from positive to negative. The complete oxide coverage of the surface is thus identified as the dominant process leading to the I_{ox} peak.

MEASUREMENTS IN THE PSL-REGIME

In the PSL-regime (i.e. before the PSL peak) the same kind of experiment was performed. The fact that current transients could be found leads to the conclusion that oxide exists even in the low voltage part of the characteristics – in contradiction to the general belief, e.g. (18), that oxidation is not involved here. This result is confirmed by IR spectroscopy (19).

If the ratio I/Q of the current I and the total charge Q contained in a transient, is plotted vs. the voltage in Fig. 3, two intersecting straight lines result. The point of intersection corresponds to the point of inflection A on the I-U-curve of Fig. 1 and the current transients before or after the inflection points have qualitatively different shapes. Before the inflection point is reached, transients immediately start with their maximum value and $dI/dt < 0$. At the point of inflection the transients form a plateau ($dI/dt = 0$) for the first time followed by peaks ($dI/dt > 0$). If the transients represent the oxide thickness distribution, the evolution of a peak indicates that for voltages above the inflection point voltage a significant amount of the oxide is thick enough to resist the etching agent for some longer time which hinders current flow. This will be discussed in more detail later.

MEASUREMENTS IN THE OSCILLATION REGIME

In this regime, starting on the downwards slope of the second peak (I_{ox}), damped or sustained oscillations of the current (or, under galvanostatic conditions, voltage) are observable. Both impedance data and current transients show independently that the oxide thickness oscillates with the current (6, 15). Simulations based on the current burst model (6, 15) reproduced not only the current oscillations, but also the impedance and transient measurements in detail. It is useful to summarize the essentials of the model briefly as a base for the measurements presented here.

In the oscillation regime the Si surface is completely covered with oxide at any time and all current must flow through this oxide layer. The voltage then drops mostly across the oxide layer and (without current; i.e. in the low-current phase of the oscillations) the field strength within the oxide increases steadily because the oxide is thinned by the HF.

Around a critical field strength (approximately 3V/nm) current bursts nucleate with increasing probability inducing some kind of ionic oxide break through, and strongly localized oxide growth occurs until the local field strength quenches the current burst with increasing probability and the pure etching phase starts again. This is the basic oscillation mechanism inherent in the current burst model and the oscillation frequency f is given by the average duration τ_{CB} of a current burst to $f = 1/\tau_{CB}$. Macroscopic oscillations require a synchronization mechanism correlating the phases of the local oscillators or current bursts in an area, called a **domain**, commensurable with the specimen size. A next neighbor interaction mediated by the oxide "bumps" formed by individual current bursts provides the necessary phase correlation within one domain; if the density of current bursts exceeds a certain percolation threshold, the **correlation length** of this process, which defines the domain size, increases rapidly and stable macroscopic oscillations result. Below the percolation threshold, the correlation length or domain size is decreasing with decreasing voltage and many small domains oscillate independently. Since the domains are not phase coupled, the total current will be constant but noisy with a power spectrum of the noise showing a pronounced maximum at the oscillation frequency; this was a prediction of the current burst model that has indeed been observed by Chazalviel et al. who first proposed oscillating domains (14, 20, 21).

Current transient measurements reported in (15) and corresponding measurements in this work always show a reduced total suboxide charge in the active phase of an oscillation, i.e. at high currents. This is interpreted by a rapid loss of the suboxide charge through the open channels at the time of the voltage switching which will not be recorded because the system needs some time before the current transient measurements can start. If the inflection point on the ascending part of the I_{ox} peak indeed marks the onset of a closed oxide layer, with increasing current an increasing number of current bursts that do not contribute to the suboxide charge must be present at any time; the $Q(U)$ curve must go down again after reaching a maximum around the inflection point.

Oscillating domains of small size, if started at the same time, will have some phase coherence which then randomizes with a characteristic time constant τ_R which gives the decay time of damped oscillations that must result. Synchronization of domains can simply be achieved by starting them all at the same time, i.e. by switching directly to a voltage of the oscillation regime before the onset of stable oscillations. Such an experiment is shown in Fig. 2a in (17). For lower voltages the current drops from higher values to an equilibrium current. The first signs of oscillations occur at a voltage of 1.7 V (under these experimental parameters) slightly undershooting the average value. Again this voltage corresponds to the point of inflection on the I-U-curve and, since d^2I/dU^2 is negative from the starting point of oscillations, it must be concluded that oscillations (i.e. formation of large domains) are a current supporting mechanism.

The damping time constant τ_R as obtained from the envelope of the damped oscillations, and $1/f$ (identified as τ_{CB} in the current burst model) vs. the voltage, is shown in Fig. 4. A linear dependence is found. While the linear increase of τ_{CB} is due to the increase of the average oxide thickness with voltage as expected (6, 15), the linear dependence of the damping constant has not been observed before; it shows again the linear dependence of the coupling mechanism on the applied voltage.

In addition the amplitude of the first extrema of a damped oscillation can be taken as a measure of the coupling strength between the oscillating domains. A linear relationship is found (cf. Fig. 3 in (17)) when it is plotted vs. voltage. This again indicates a direct increase of the coupling strength with the voltage.

Since there is no direct coupling between domains, the phase coupling of domains simply reflects the phase coherence in time of a single domain. The current oscillations within a given domain result from stochastic processes; so the phase of the current maximum will eventually randomize for a given domain, and it is this effect that randomizes the phases between domains. The coupling strength between domains as discussed above thus directly reflects the coupling strengths of current bursts within a domain.

At low potentials where no damped oscillations appeared, there is still a considerable noise of the current, decreasing with decreasing coupling strength (and thus smaller correlation lengths, i.e. more domains) as expected. While the autocorrelation spectra of this noise does indeed contain a strong peak at $t - t' = 1/f$, the presence of the oscillation frequency at nominally constant currents can be found in a direct way since a system containing oscillating domains can be expected to show some kind of resonant behavior following external excitations at the proper frequency. Experiments to explore this avenue were performed in two closely related ways.

In a first set of experiments a sinusoidal voltage with an amplitude of 25 mV and an adjustable frequency f_{ex} around the oscillation frequency f_U = 18-19 mHz was superimposed on the constant voltage U which in Fig. 2a in (17) caused damped oscillations with f_U. The result for U = 2.3 V and several signal frequencies around f_U is shown in Fig. 6. a) and b). The current response clearly shows a pronounced maximum at the system frequency f. A resonant behavior of this kind was also obtained at other voltages and frequencies.

In a related set of experiments the FFT impedance spectrometer was used in an unconventional way. After the damped oscillations disappeared, a perturbation signal was applied, consisting of 43 sinusoidal signals with identical amplitudes and a bandwidth that included the frequency f_U of the macroscopic oscillations. The response was not evaluated as impedance but plotted directly. The resulting spectra (similar to those in Fig. 7) not only show significant peaks around the system frequency f_U, but additionally extremely nonlinear response peaking at f_U, too. This means that many frequencies not contained in the perturbation signal were generated – as one would expect from a stochastic and therefore intrinsically non-linear resonance. If the voltage is lowered or raised, the peaks shift to smaller or longer periods, respectively.

The nonlinear peak could be observed in the spectra of Fig. 7 at voltages as low as 1.2 V, i.e. at potentials before the I_{ox}-peak where (under these experimental parameters) not even damped oscillations were obtainable. Fig. 5 shows that the expected linear dependence between voltage and the resonant period holds in this region, too.

It is worthwhile to point out that in conventional FFT impedance spectroscopy the non-linear behavior as expressed in the strong peak at f would be disregarded and excluded from data evaluation, while here it is the phenomenon sought after. In most conventional impedance measurements, however, this peak would not appear because the frequencies in the perturbation signal usually are much higher.

VOLTAGE OSCILLATIONS

Voltage oscillations occur at constant currents within a certain window. They have a more complicated shape than the current oscillations (Fig. 8b) but the electrode is still covered by a closed oxide layer at all times. It is noteworthy that at the low HF concentrations used here, stable oscillations were obtainable only by switching the current to lower values after a certain oxide thickness was reached. If this current is too low the voltage will drop and no oscillations can start. At higher currents oscillations occur (as a closed oxide layer can be formed), but the mean voltage steadily rises.

As in the case of the current oscillations the reason for these oscillations can be found in the current burst model as follows: Within a current burst cycle the resistance R_{CB} changes as a function of the current burst phase. If current bursts are not synchronized (random phase approximation), an over all resistance R of the Si-electrolyte interface is found which is calculated by

$$\frac{1}{R(t)} = {}_{CB} \left\langle \frac{1}{R_{CB}(t)} \right\rangle = N \left\langle \frac{1}{R_{CB}} \right\rangle = const. \qquad [1]$$

For potentiostatic as well as for galvanostatic control a constant non oscillating current, respectively voltage will be measured. On the other hand, if one percolating domain exists, Eq. [1] changes to

$$\frac{1}{R(t)} = {}_{CB} \frac{1}{R_{CB}(t)} = N \frac{1}{R_{CB}(t)} \qquad [2]$$

Consequently for potentiostatic control current oscillations are measured while for galvanostatic control the voltage must oscillate in order to ensure a constant current across the Si-electrolyte interface. This change in the ohmic resistance of the circuit is directly measured with impedance spectroscopy (cf. Fig. 8d).

As derived from the capacitance results in Fig 8a) the oxide thickness is nearly constant or only slightly increasing. The peaks in curve a) coincide with strong changes in the potential where the stationarity for impedance analysis may not be fulfilled and may be artifacts of the measurement technique.

In contrast to current oscillations (6, 15) the voltage oscillations are not connected to essential changes in the oxide thickness. The difference in the serial resistance can be explained by a periodically changing number of oxide breakthroughs as proposed by the current burst model (6, 15).

DISCUSSION

From the measurements presented, and from supporting evidence contained in (17), a first tentative understanding of the *I-V*-characteristics emerges which includes the attached phenomena, expressed e.g. in the two maxima j_{PSL} and j_{ox}, but also in the inflection points and in pore formation.

The measurements presented indicate that the points of inflection are more important for an understanding than the maxima of the current. Inflection points generally indicate that mechanisms hindering (or promoting) further increase of the current with increasing voltage become noticeable while the current itself still increases (or decreases). The maxima then simply signify that two opposing mechanisms are present at comparable strength. It is thus important to understand the mechanisms causing the inflection points.

As discussed above, the oxide coverage of the surface is complete at the point of inflection C in Fig. 1 on the ascending part of the I_{ox}-Peak, and the hindering mechanism indicated is the more difficult nucleation of current bursts through a closed oxide. However, even so d^2I/dU^2 is negative, dI/dU is positive - the current still rises for a while. The reason for this may be sought in an increasing oxide roughness along the ascending part of the I_{ox} peak. This increases the etching rate because the area per oxide volume that is exposed to the HF increases. The intrinsic time constant τ_{CB} decreases and the charge passed per time in a current burst (i.e. the current) increases. Essentially, the removal of the oxide determines the current and optimizing the roughness will minimize the required etching time.

The fourth inflection point on the descending branch of I_{ox} indicates the formation of appreciable oscillating domains which render current flow easier. This is automatically the case if the characteristic is non-linear, which allows oscillations to pass more power at a given voltage than at constant current. The current, however, is still decreasing because the now dominant effect of the reduced nucleation probability of current bursts through closed oxide (that caused the third inflection point) is still dominant.

A similar argument may hold for the first point of inflection point in the PSL-regime. The ascending part of the characteristics simply indicates an increase of the current burst nucleation probability, the current will increase exponentially as long as the area covered with current bursts is small compared to the total area. Since current bursts tend to cluster and then to form synchronized domains, macropores may be formed if the domains stay in one place long enough. Pre-defined nuclei will pin down domains, it thus can be predicted that macropore formation for p-type Si in aqueous electrolytes at low current densities will be much easier with induced nucleation and may not happen at all without. The current density in the domains, or within the macropores if formed, is the maximum current transferable under those conditions. The maximum of the external current would be reached if the whole surface is covered with domains or macropores. Again, the current limiting factor is essentially the removal of the oxide. The inflection point for this case only would indicate the beginning of current burst correlation, i.e. the formation of domains.

The system, however, has an option not yet included. Increasing the oxide roughness and thus dissolution rate would give rise to a current increase and, as in the case discussed before, this can be achieved by destroying the correlation between current bursts and replacing it with an anti-correlation. Each current burst than acts independently of its neighbors and nucleates as soon as possible - a rough surface would result. However, Si is a semiconductor, and the first pores dug by individual current bursts must never meet or coalesce because the quantum wires (or better quantum dots) formed if two micropores come close cut off the carrier supply and force the current burst apart. Increasing the voltage and thus the current then can only increase the porosity – pores must divide because only one burst is allowed per pore. A limit is reached at some maximum porosity when all of the Si left is a quantum wire, defining the j_{PSL} peak.

The inflection point thus marks the region where micropore formation may become favorable. While it has never been carefully measured, it appears to be close to the maximum j_{PSL} for low HF concentrations, but quite distinct for lower concentrations. Highly porous micropores thus should be found at high current densities and high HF concentrations, while the opposite conditions would favor macropores especially if domain pinning by induced nucleation is used – in accordance with experimental results, (1, 2).

This interpretation also may be used to understand the results shown in Fig. 3. While the two intersecting straight lines meeting at the point of inflection are rather well defined, indicating some simple explanation, it is not yet obvious. The ascending line indicates a linear increase in the current burst oxide thickness and a linear decrease in the ratio between oxide coverage and current. Combining both information, the oxide covered areas do not hinder additional current in this regime of the *I-U*-curve. At the crossover to the descending line free (not oxide covered) surfaces become rare, i.e. additional current flow is hindered effectively. Up to now there exists no convincing argument why a linear relationship with potential in the descending part is measured, but the abrupt change at the crossing point of both lines indicates that drastic changes in the surface morphologies may be expected at the point of inflection A.

The second point of inflection (on the downward slope of the PSL-peak) is the only one that could not yet be tied to a prominent feature of measurements as described. The slope changes from negative to positive and thus the appearance of a current supporting mechanism is indicated while a current hindering mechanism (the loss of oxide "roughness" after the micropores disappeared) still prevails. It is possible that this inflection point indicates the start of current burst nucleation through the oxide, rendering oxide covered ("dead") areas ready for charge transfer at an earlier time. There is, however, no compelling direct evidence for this suggestion.

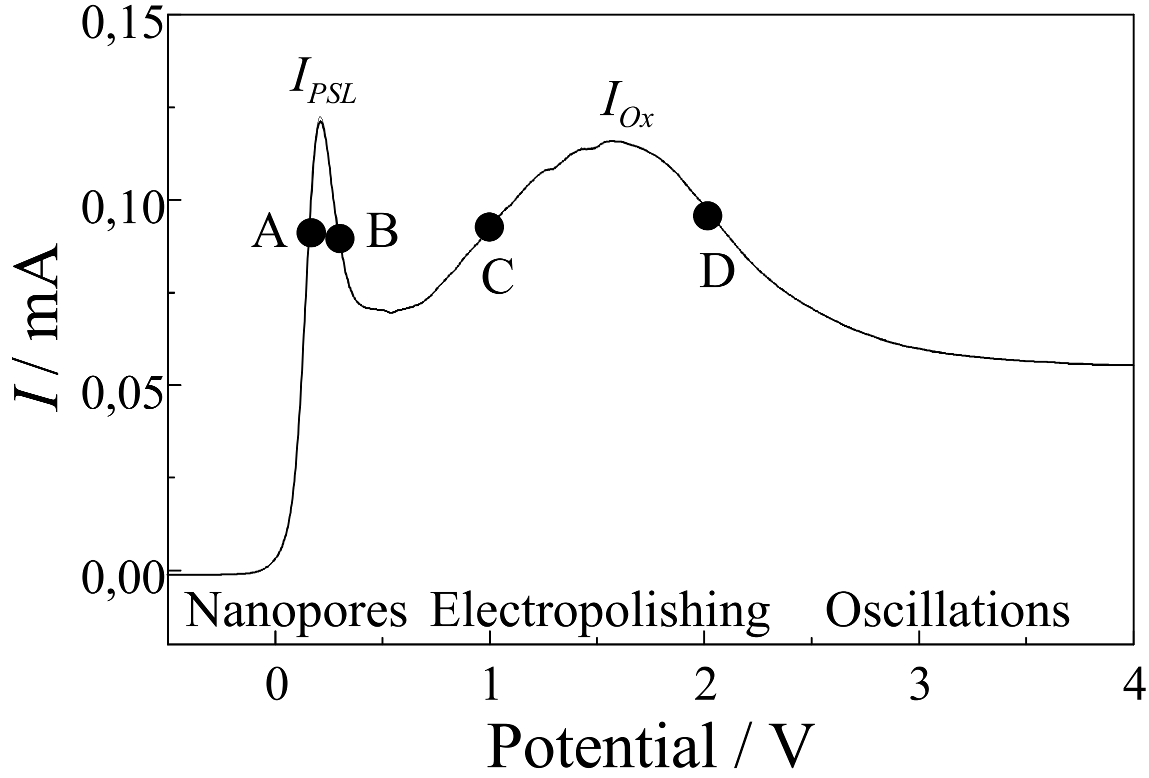

Fig. 1: Typical current-voltage characteristic for p-Si. The four points of inflection (IP) are marked.

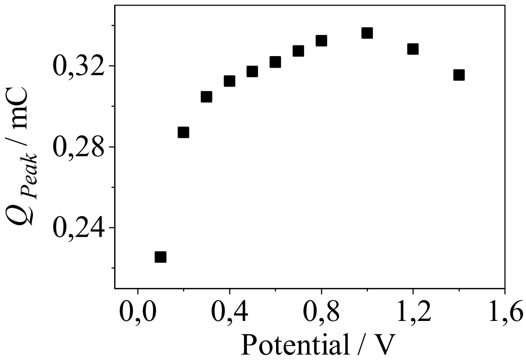

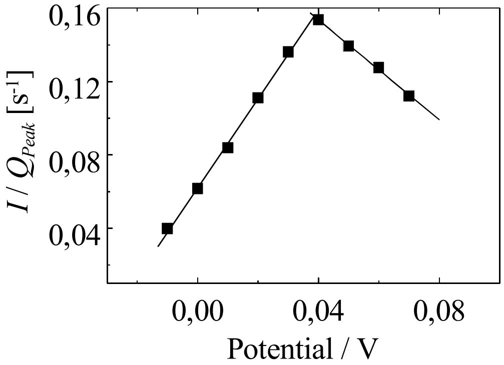

Fig. 2: Integrated transient peak yields suboxide charge in the electropolishing regime. The peak coincides with IP C in Fig.1

Fig. 3: Ratio of current and respective suboxide charge in the PSL regime. The maximum coincides with IP A in Fig. 1

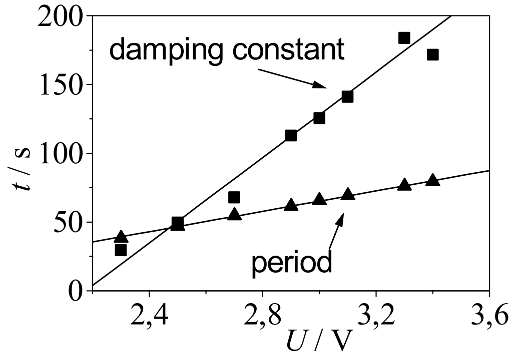

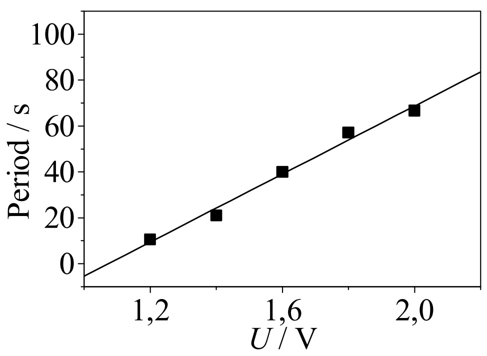

Fig. 4: Oscillation period and damping constant vs. the voltage. The damping constant was obtained by fitting the exponential decay of the oscillation curves.

Fig. 5: The period of the oscillating domains vs. voltage measured from the resonance experiments.

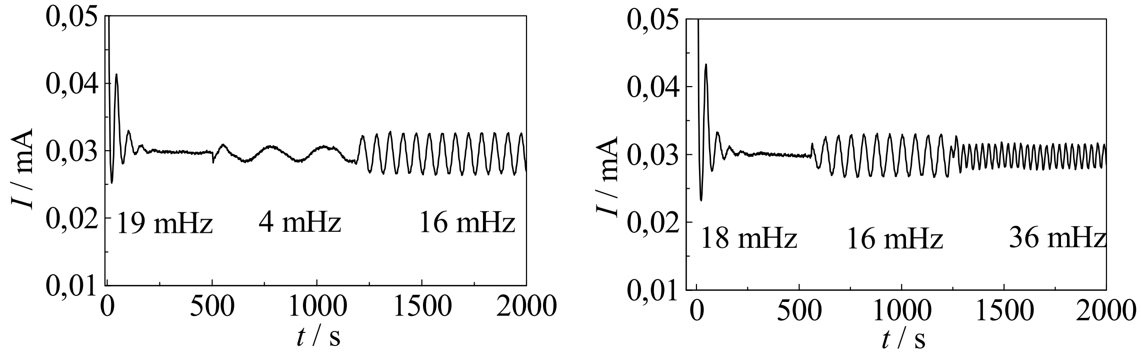

a)

b)

Fig. 6: Current response to external excitation after the original oscillations (at the frequency indicated) disappeared a) External excitations with frequencies below, b) with a frequency above the resonance frequency.

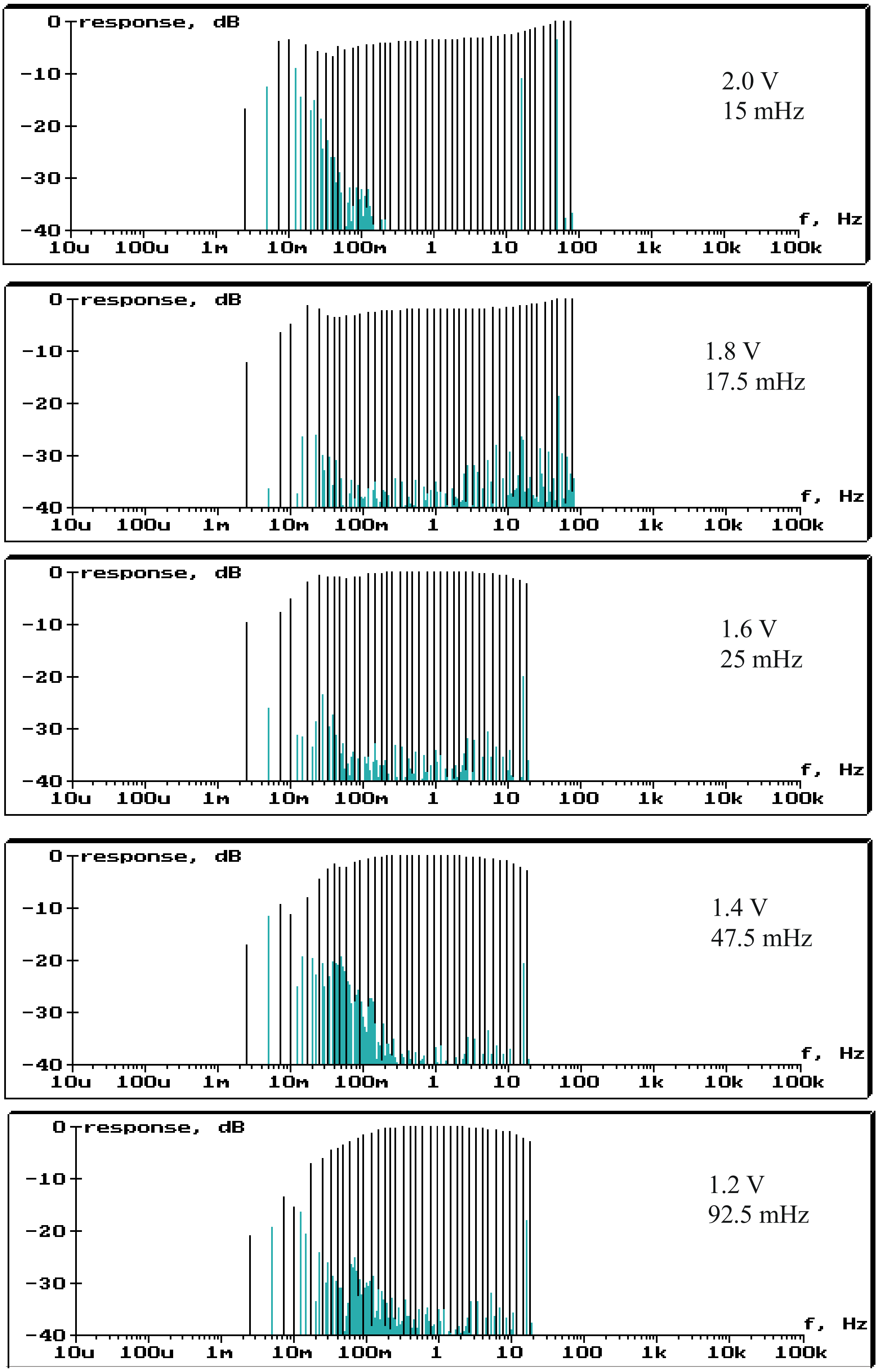

Fig. 7: Current response to a signal with many frequencies as a function of the voltage. The resonance frequency as deduced from the peaks is indicated in all figures.

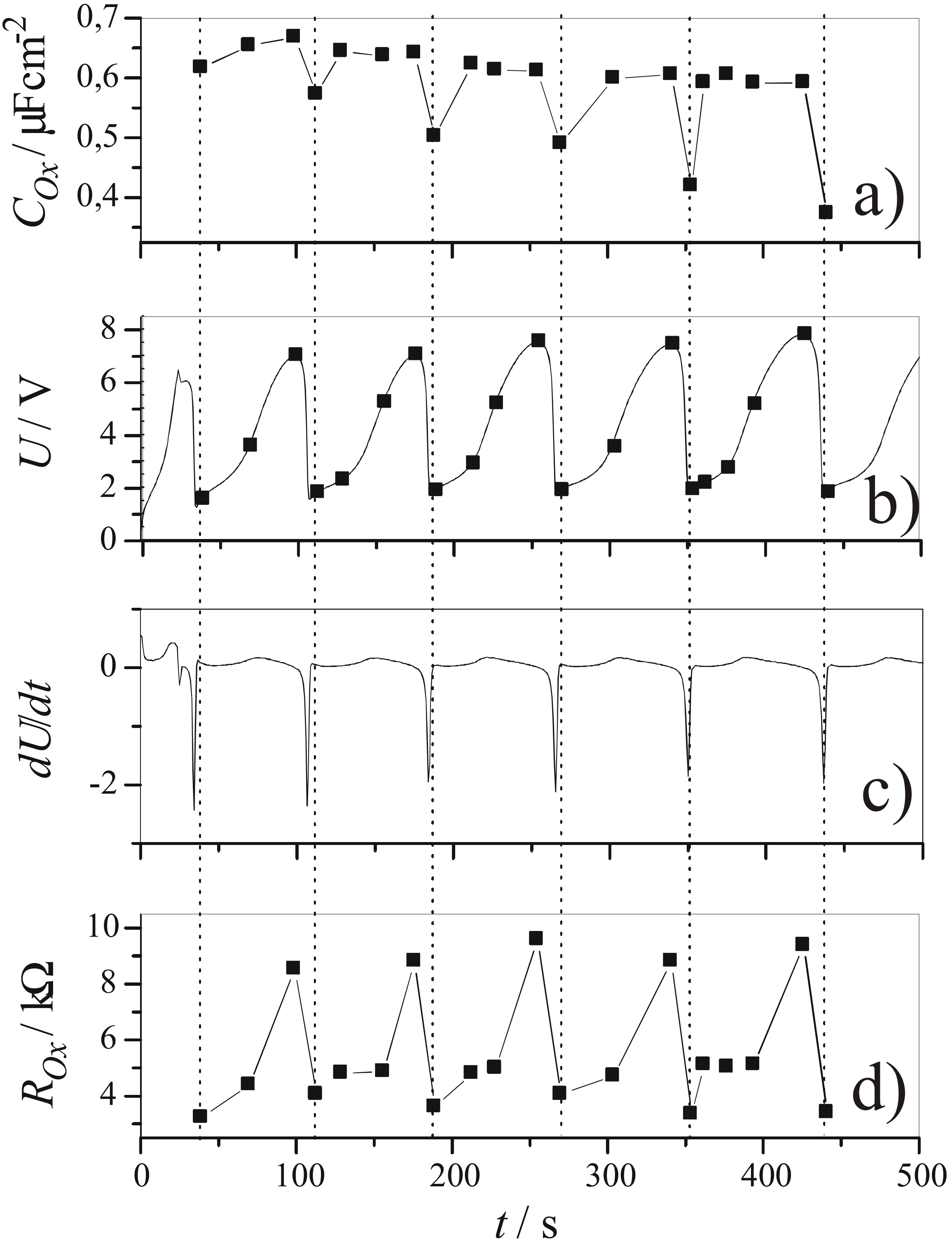

Fig. 8:Measurements for voltage oscillations under galvanostatic conditions. a) Oxide layer capacity, b) Oscillation curve, c) Time derivative of the Voltage, d) Oxide layer resistance.

REFERENCES

1. V. Lehmann, H. Föll, J. Electrochem. Soc., 137, 653 (1990)
2. H. Föll, Appl. Phys. A, 53, 8 (1991)
3. D. R. Turner, J. Electrochem. Soc., 107, 810 (1960)
4. V. Lehmann, U. Gösele, Adv. Mat., 4, 114 (1992)
5. L.T. Canham, Appl. Phys. Lett., 57, 1046 (1990)
6. J. Carstensen, R. Prange, H. Föll, J. Electrochem. Soc.,146, 1134 (1999)
7. H. Föll, J. Carstensen, M. Christophersen, G. Hasse, to be published Phys. Stat. Sol. (a) 182, (2000)
8. M. Christophersen, J. Carstensen, H. Föll, to be published Phys. Stat. Sol. (a) 182, (2000)
9. Carstensen, M. Christophersen, G. Hasse, H. Föll to be published Phys. Stat. Sol. (a) 182, (2000)
10. G.S. Popkirov, R.N. Schindler, Electrochimica Acta, 38 (7), 861 (1993)
11. G.S. Popkirov, R.N. Schindler, Rev. Sci. Instrum., 63,(11), 5366 (1992)
12. M. Matsumara, S.R. Morrison, J. Electroanal. Chem., 147, 157 (1983)
13. J. Rappich, H.-J. Lewerenz, J. Electrochem. Soc., 142 (4), 1233 1995
14. F. Ozanam, J.-N. Chazeviel, A. Radi, M. Etman, Ber. Bunsenges. Phys. Chem., 95 (1991)
15. J. Carstensen, R. Prange, G. S. Popkirov, H. Föll, Appl. Phys. A., 67, 459 (1998)
16. J. Carstensen, R. Prange, H. Föll, J. Electrochem. Soc.,146, 1134 (1999)
17. G. Hasse, J. Carstensen, G. S. Popkirov, H. Föll, Mat. Sci. Eng. , B 69 – 70, 188 (2000)
18. H.J. Lewerenz, Chem. Soc. Rev., 26, 239 (1997)
19. A. Beladi, M. Safi, F. Ozanam, J.-N. Chazalviel, O. Gorochov, J. Electrochem. Soc., 146 (7), 2659 (1999)
20. F. Ozanam, N. Blanchard, J.-N. Chazalviel, Electrochim. Acta, 38 (12), 1627 (1993)
21. J.-N. Chazeviel, F. Ozanam: J. Electrochem. Soc., 139 (9), 2501 (1992)